RESEARCH ARTICLE

Cosmological Evolution: A Study of Transition Periods

Bob Osano [1,2,*]

[1] Cosmology and Gravity Group, Department of Mathematics and Applied Mathematics, University of Cape Town, Rondebosch 7701, South Africa
[2] Centre for Higher Education Development, University of Cape Town, Rondebosch 7701, South Africa

Abstract

This study investigates two transitions in cosmology: radiation-matter and matter-dark energy. For each transition, a parameter χ is employed, representing the ratio of the two energy densities involved in the relevant transition. The focus on the second transition is motivated by the need to understand an accelerating universe. In examining potential cosmic acceleration due to dynamic dark energy, a dynamical equation of state for dark energy is considered in terms of the ratio χ and the deceleration parameter q. The resulting system of equations is analyzed by varying parameters to investigate their influence on the evolution of the universe. To achieve cosmic acceleration, the equation of state for dynamic dark energy (denoted ω) must satisfy $\omega < -2/3$ at the matter-dark energy transition, corresponding to $\omega < -0.47$ at present.

Keywords: cosmological transitions, dark energy dynamics, deceleration parameter, friedmann equations, equation of state.

Submitted: 09 September 2025
Accepted: 18 September 2025
Published: 23 November 2025

Vol. 1, **No.** 2, 2025.
10.62762/JNSPM.2025.159712

***Corresponding author:**
Bob Osano
bob.osano@uct.ac.za

1 Introduction

The fact of cosmic acceleration, by now strongly established by many observations [1–3], remains a puzzling phenomena theoretically. It was once thought that the ΛCDM model framework for cosmology was definitive, and that want reamined efforts to refine the estimates of key parameters: h, Ω_m, Ω_b, Ω_Λ, Ω_r, Ω_ν, $\Delta^2\mathcal{R}(k*)$, n, r, and τ [4]. These represent, respectively, the Hubble parameter, matter and baryon densities, the cosmological constant, radiation density, neutrino density, the amplitude and spectral index of primordial fluctuations, the tensor-to-scalar ratio, and the optical depth to reionization. What has transpired, though, is that attempts to obtain better estimates of these values using different data sets and methodologies have not converged, and in some cases have challenged the Λ CDM framework itself. However, efforts to constrain these values using other datasets and approaches have not been uniformly consistent, and at times have even led to some degree of tension with the ΛCDM paradigm [5–7]. The most famous cases being the continuing tension in the Hubble constant and the more global question of the late-time cosmic acceleration [8]. Nevertheless, despite all these difficulties, studies of the earlier epochs (starting from the dominance of radiation and followed by matter) significantly improved our view of the past history of the universe. During the radiation

Citation
Osano, B. (2025). Cosmological Evolution: A Study of Transition Periods. *Journal of Numerical Simulations in Physics and Mathematics*, 1(2), 67–75.

domination epoch, baryons were tightly coupled to photons and could not form small-scale clustering under the influence of radiation pressure. Cold dark matter perturbations could only grow logarithmically, suppressing structure formation at this stage [9]. When the universe became matter-dominated, the suppression was lifted, and small-scale perturbations could grow more easily. The crossing took place at matter-radiation equality. Modes that crossed the horizon earlier, during radiation domination, suffered from the most severe suppression, and that is why the power spectrum declines in small scales. The feature appears on the horizon at matter–radiation equality. As the location of this turn-over is determined by the matter density and related parameters, it represents an excellent cosmology probe [10, 11].

The main goal of this paper is to explore if a more recent transition (matter domination $\rightarrow$ dark energy domination) may give rise to a similar signature. With the discovery of cosmic acceleration, models with a dynamical DE component driving the expansion have drawn much attention [12–18]. Since the radiation–matter transition has played such a pivotal role in constraining cosmology, it is, of course, also interesting to ask if an analogous study of the matter–dark energy transition might be similarly illuminating. A closer look at this transition is presented in the next section, beginning with a brief recap of the basic equations that form the mathematical basis of the study.

2 Friedmann Equations

The hot Big Bang model is still considered the standard theory for describing the evolution of the universe in an early stage [19, 20]. Here, the spacetime is described by the isotropic and homogeneous Friedmann–Lema$\hat{i}$tre–Robertson–Walker (FLRW) solution of Einstein's field equations, in which the expansion is characterized by the scale factor $a(t)$ [21]. The change of $a(t)$ is determined by Friedmann equations:

$$\frac{\dot{a}^2}{a^2} = \frac{8\pi G}{3}\rho_{Tot} - \frac{k}{a^2} + \frac{\Lambda}{3}, \quad (1)$$

$$\frac{\ddot{a}}{a} = -\frac{4\pi G}{3}(\rho_{Tot} + 3p_{Tot}) + \frac{\Lambda}{3}, \quad (2)$$

where G is the gravitational constant, k denotes the spatial curvature, ρ_{Tot} is the total energy density, and p_{Tot} the total pressure. Natural units with $c = 1$ are adopted throughout. Inserting the Hubble parameter $H = \dot{a}/a$, equation (1) can be rewritten as:

$$1 = \frac{8\pi G}{3H^2}\rho_{Tot} - \frac{k}{a^2H^2} + \frac{\Lambda}{3H^2}. \quad (3)$$

This representation highlights the fractional contributions of the various components to the total energy density.

The density parameter Ω, widely used in cosmology [22], is defined as the ratio of the actual density ρ to the critical density ρ_c given by the FLRW model. This ratio governs the interpretation of the geometry: $\rho = \rho_c$ corresponds to a flat universe, while earlier models without a cosmological constant used it to distinguish between open and closed geometries.

3 Interactions and the evolution of total energy density

Attention is turned to the evolution of the total energy density in an FLRW universe containing several components: radiation (ρ_r), ordinary/baryonic matter (ρ_m), and dark matter (ρ_{DM}). To facilitate this discussion, $\rho_M = \rho_{DM} + \rho_m$ is defined as the combined matter sector. Two forms of dark energy are also distinguished: a dynamic part, ρ_{DDE}, and a non-dynamic contribution, ρ_{NDE}. This separation is useful since the entity often described as "dark energy" may consist of different pieces. In our framework, ρ_{DDE} interacts with dark matter. The formulation, nevertheless, allows this interaction to be switched off if need be. A natural question to ask is whether such couplings are significant enough to alter the evolution of ρ_{Tot}. Other interactions may also occur, for example, the interaction between radiation matter could arise through ionisation processes. Highly energetic photons or particles may eject electrons from atoms, leaving partially ionised matter whose growth history differs from that of neutral matter or radiation alone. The relevance of such processes is whether they appreciably modify the time evolution of ρ_{Tot}.

In this study, the dark-sector components are modelled as perfect fluids described by a barotropic equation of state. The interactions considered are non-dissipative, so there is no need to invoke the extended theory of relativistic thermodynamics [23–27]. The corresponding energy–momentum tensor takes the familiar form

$$T^{\nu\mu}_{Tot} = (\rho_{Tot} + p_{Tot})u_\nu u_\mu + p_{Tot}g_{\nu\mu}, \quad (4)$$

which satisfies the conservation law $\nabla^\nu T^{\nu\mu}_{Tot} = 0$. Each density evolves according to its own equation but may exchange energy through interaction terms. To capture such effects, hypothetical couplings are introduced between selected pairs of species, chosen in line with cosmological epochs. Specifically, radiation–matter interaction is denoted Q_{rm}, while matter–dark energy interaction is Q_{ME}. No coupling between dark matter and baryons is included [28]. The evolution equations then read:

$$\begin{aligned}
\dot{\rho}_r &= -3H(1+\omega_r)\rho_r + Q_{rm}, &(5)\\
\dot{\rho}_m &= -3H(1+\omega_m)\rho_m - Q_{rm}, &(6)\\
\dot{\rho}_{DM} &= -3H(1+\omega_{DM})\rho_{DM} + Q_{ME}, &(7)\\
\dot{\rho}_{DDE} &= -3H(1+\omega_{DDE})\rho_{DDE} - Q_{ME}, &(8)\\
\dot{\rho}_{NDE} &= 0. &(9)
\end{aligned}$$

The main focus is the transition behaviour between epochs. Before analysing these dynamics, it is useful to clarify the meaning of a dominant matter type.

4 Dominant matter type

Although domination requires one density to be higher than the rest, the upper limit is chosen such that it exceeds all the remaining combined [29]. In the context of this analysis, a matter type is considered dominant if its energy density is 50% of ρ_{Tot} or higher. In principle, this definition ensures that the acceleration is attributed to the dominant matter type in the epoch under consideration.

5 Radiation-Matter transition

The transition from radiation domination to matter domination is characterised by radiation and matter constituting the greater proportion of the cumulative energy density. As previously mentioned, this is interpreted as the dominant density, which accounts for at least half of the total energy density. A new parameter is defined to study this transition period. To this end, subtracting equation (1) from equation (2), setting $8\pi G = 1$ and $\kappa = 0$, and expressing the resultant equation in terms of the Hubble parameter using the system of equations (5) yields

$$\begin{aligned}
\dot{H} &= -\frac{1}{2}[(1+w_r)\rho_r + (1+w_m)\rho_m)\\
&\quad +(1+w_{DM})\rho_{DM}) + (1+w_{DDE})\rho_{DDE}], \quad (10)
\end{aligned}$$

where H has the dimension of time. A transition epoch involves the preceding and the succeeding dominant energy densities. For example, the radiation-to-matter transition has radiation as preceding and matter as succeeding. Equation (10) can be rewritten by factoring out the preceding energy density such that

$$\begin{aligned}
\dot{H} &= -\frac{1}{2}\rho_r\Big[(1+w_r) + (1+w_m)\frac{\rho_m}{\rho_r})\\
&\quad +(1+w_{DM})\frac{\rho_{DM}}{\rho_r}) + (1+w_{DDE})\frac{\rho_{DDE}}{\rho_r}\Big]. \quad (11)
\end{aligned}$$

The ratios of energy densities of the subdominant species are taken as small in comparison to ρ_M/ρ_r and hence can be set to zero. In principle, the subdominant densities do not vanish but have a negligible contribution to the Hubble parameter (11), and as such,

$$\dot{H} \approx -\frac{1}{2}\rho_r[(1+w_r) + (1+w_m)\frac{\rho_m}{\rho_r})]. \quad (12)$$

It is the last term in equation (12) that provides a hint for defining a new parameter.

5.1 A density ratio parameter

A new parameter is defined as the ratio:

$$\chi_{rm} = \frac{\rho_m}{\rho_r}. \quad (13)$$

Although $0 < \chi_{rm} < \infty$, the focus is on the dynamics around matter-radiation equality, which, in terms of the new parameter, occurs around $\chi_{rm} = 1$. For example, the horizon size sets the position of the peak of the matter power spectrum at the epoch of matter-radiation equality [31]. The position of the first peak is consistent with a flat universe.

A variant of equation (12) is given in the dark matter - dark energy transition epoch section. For now, taking the time derivative of χ_{rm} and using equations (5 and 6) yields

$$\dot{\chi}_{rm} = -\Theta(w_m - w_r)\chi_{rm} - \frac{Q_{rm}}{\rho_r}(1+\chi_{rm}), \quad (14)$$

where $w_m = 0$ and $w_r = 1/3$.

It is shown below that equation (14) is coupled to other equations. Before addressing this, the interaction term in equation (14) is discussed. The material whose densities are considered here may experience different interactions, but not including those that may change the nature of interacting material (e.g.

chemical). The effect of the interaction could be quantified by detailing the proportion of materials undergoing interaction. For this reason, the interaction term Q_{rm} may be expressed as a proportion of the ratio χ_{rm}. i.e. $Q_{rm} = \psi(t)\chi_{rm}$, where the highest interaction occurs at equality ($\chi_{rm} = 1$), for that is when the largest percentage of the two fluids may experience interaction. Even though the system considered is nonlinear and not time-invariant, the product $\psi(t)\chi_{rm}$ mimics a transfer function. Equation (14) takes the simple form:

$$\dot{\chi}_{rm} = -\Theta(w_m - w_r)\chi_{rm} - \frac{\psi\chi_{rm}}{\rho_r}(1 + \chi_{rm}). \quad (15)$$

This is one of the main equations in the radiation-matter transition epoch. The other relevant equations are the evolution equation for radiation given by equation (6) and equation (12). Let $X = \chi_{rm}$, $Z = 1/\rho_r$, and apply $w_r = 1/3$, $w_m = 0$; the system can then be expressed in the following compact form.

$$\begin{aligned} \dot{X} &= HX - \psi XZ(1 + X) && (16)\\ \dot{Z} &= 4HZ - \psi XZ^2 && (17)\\ \dot{H} &= -\frac{1}{Z}\left(\frac{X}{2} + \frac{2}{3}\right). && (18) \end{aligned}$$

This generic system of equations enables us to study the transition from radiation to matter domination. In fact, in standard particle cosmology [32], one comes across a similar ratio correlation of the form $1 + \rho_\nu/\rho_\gamma$where ρ_ν is the density of neutrinos and ρ_γ is the photon density.

It is emphasised that the assumptions and ansatz used in obtaining the numerical solution to this system are arbitrary and chosen for illustration purposes. The function ϕ is taken to be cosmic time-dependent with a maximum value at t_{eq}, or when $\chi_{rm} = 1$. The ansatz $\psi(t) = e^{-t^2}$ is employed, with $t_{eq} = 0$ corresponding to matter-radiation equality. The following initial conditions are used to obtain the numerical solutions presented in Figures 1 and 2: $X_{rm} = 0.4$, $Z = 2$, and $H = 0.67$.

5.2 Results and Analysis

It is observed that such hypothetical interactions given by Q_{rm} influence the early-time behaviour of the universe, specifically close to equality. In this work, the analysis is intentionally restricted to the initial form of the interaction term and an exponential ansatz,

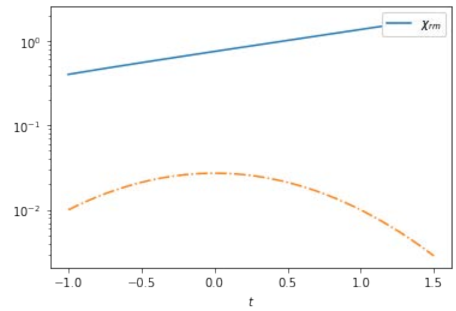

Figure 1. *This plot shows how χ_{rm} and ψ grow with cosmic time. The scale is normalised such that $t_{eq} = 0$.*

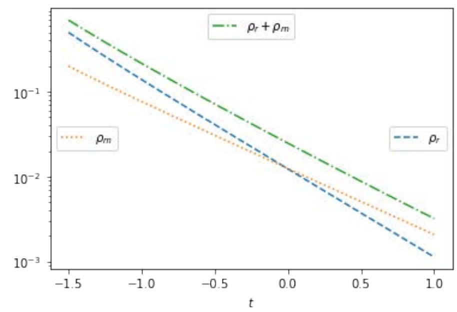

Figure 2. *The plot shows the devlopment of ρ_r, ρ_m and the sum $\rho_m + \rho_r$ plotted against cosmic time. A logarithmic scale is used on both axes. The plots are normalised such that $t_{eq} = 0$ (equivalently $\chi_{rm} = 1$).*

which is considered a source of driving forces for the interaction term. The EoS of the two competing densities are determined in this case. The primary parameter, χ_{rm}, increases with cosmic time as seen in Figure 1. The two densities grow as expected around $\chi_{rm} = 1$. The interaction term dictates the duration to reach equality. In terms of physics, this would impact structure formation. Structures smaller than the horizon experience stunted growth during radiation domination. A delay in time to equality affects an even greater percentage of such structures. As the universe expands, the radiation density drops faster than matter as indicated in Figure 2. This is due to the redshifting of photon energy leading to an estimated crossover or matter-radiation equality ($\chi_{rm} = 1$) at about 50,000 years after the Big Bang. Beyond $\chi_{rm} = 1$, fluctuations in all dark matter potentially grow unimpeded and create kernels into which the baryons can later fall. The turnover in the matter power spectrum is induced by the particle horizon at this epoch. This turnover can be measured in large redshift surveys [31]. The procedure and analysis in this section set the foundation for studying the matter-dark energy transition, where the dynamic dark energy EoS is unknown. Let us now turn to this transition.

6 Matter-Dark energy transition

From equation (10), the dark matter energy density is factored out, and density ratios that are negligible compared to ρ_{DDE}/ρ_M near dynamic matter–dynamic dark energy equality are ignored. These considerations yield

$$\dot{H} = -\frac{1}{2}\rho_M[(1+w_M)+(1+w_{DDE})\frac{\rho_{DDE}}{\rho_M})]. \quad (19)$$

As in the previous section, a new parameter is defined.

$$X_{ME} = \frac{\rho_{DDE}}{\rho_M} \quad (20)$$

The two dominant energy densities in this epoch are ρ_{DDE} and ρ_M (the combination of dark matter and matter).

6.1 Deceleration parameter

In terms of the Hubble parameter, the deceleration parameter takes the form

$$-(q+1) = \frac{\dot{H}}{H^2}, \quad (21)$$

with $q+1>0$ signifying a decelerated expansion and $q+1<0$ an accelerated expansion. Using equations (19) and (1) we find,

$$-(1+q) = -\frac{3}{2}\left(\frac{1}{1+\chi_{ME}}\right)\Big[1 + (1+\omega_{DDE})\chi_{ME}\Big], \quad (22)$$

where the ratio of all other densities, apart from that of dynamic dark energy to the combined matter, has been neglected. This is motivated by our intentions to study dynamics in the transition epoch where the two competing densities drive the universe's expansion. It will be noted, from equation (22) that

$$q = \frac{3}{2}\left[\frac{1+(1+\omega_{DDE})\chi_{ME}}{(1+\chi_{ME})}\right] - 1. \quad (23)$$

It can be seen from equations (23) that at equality, $\chi_{ME}=1$, that $\omega_{DDE}<-2/3$ implies accelerated expansion. On the other hand, if the dynamic dark energy mimics the cosmological constant $\omega_{DDE}=-1$, $X=0.5$ is sufficient to induce accelerated expansion. Investigations of the Pade model [37] seem to favour a positive deceleration parameter, which is inconsistent with observation results elsewhere.

In the fiducial model ($\kappa=0,\Omega_0=1$), observation data seem to prefer a value consistent with $\omega_{DE}=-0.94\pm0.1$ [45]. Lastly, Lastly, the quantity ω_{DDE} can be expressed as a function of the density ratio X and the deceleration parameter q. This might help in reconstructing the EoS of dynamic dark energy if q can be obtained from observation at a given density contrast. In particular,

$$\omega_{DDE} = \frac{(2q-1)(1+\chi_{ME})}{3\chi_{ME}}, \quad (24)$$

which is a formulation of EoS in terms of the deceleration parameter. This adds to the assortment of EoS already in literature, such as Chevallier-Polarski-Linder [33, 34], Barboza-Alcaniz [35] case and Low Correlation [36], others [30] and their comparisons to observation data[37–44].

6.2 Transition dynamics

We let $X=\chi_{ME}$ and $Z=1/\rho_M$. Differentiating equations (20) and using equations (7-9) yields the following closed system of equations.

$$\dot{X} = 3H(w_M - w_{DDE})X - ZQ_{ME}, \quad (25)$$
$$\dot{Z} = 3H(1+w_{DM})Z, \quad (26)$$
$$\dot{H} = -\frac{1}{2Z}\left[1+w_M+X(1+w_{DDE})\right], \quad (27)$$

where term Q_{rm} terms have been dropped from the system for the reason given above. The ansatz $Q_{ME}=\psi X$ can also be employed. Setting the $w_{DM}=0=w_M$[46] yields the reduced system

$$\dot{X} = -3H\omega_{DDE}X - \psi XZ \quad (28)$$
$$\dot{Z} = 3HZ \quad (29)$$
$$\dot{H} = -\frac{1}{2Z}\left[1+X(1+\omega_{DDE})\right], \quad (30)$$

with ω_{DDE} given by equation (24). This is the main system of equations in this study.

6.3 Results and analysis

To explore the matter–dark energy transition, the dynamics are studied for different choices of the deceleration parameter q. In this framework, late-time acceleration is attributed to dynamic dark energy ρ_{DDE} rather than to a cosmological constant, represented by ρ_{NDE}. The dynamic dark energy is modelled as a barotropic fluid with an equation of state (EoS) that is not fixed a priori. The EoS is re-expressed in terms of the deceleration parameter and applied to obtain the numerical system of equations in (25).

Our findings are presented in two ways. First, the behaviour of χ_{ME}, ρ_M, and ρ_{DDE} is analysed close to $\chi_{ME} = 1$ for different values of ω_{DDE}. The corresponding numerical results are shown in Figures 3, 4, and 5.

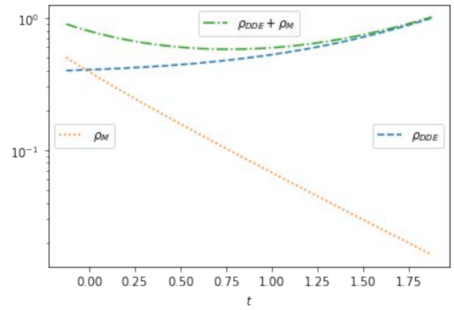

Figure 3. Growth of dynamic dark energy density for $\omega_{DDE} = -0.7$, with the potential to drive acceleration around $\chi_{ME} = 1$.

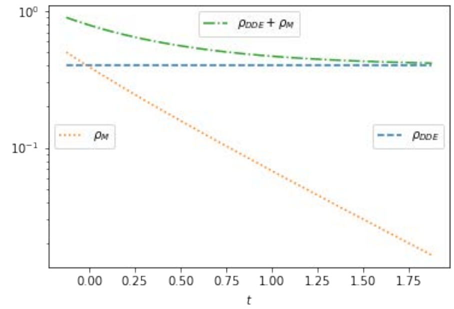

Figure 4. For $\omega_{DDE} = -1$, the behaviour is indistinguishable from ΛCDM, as expected if the cosmological constant controls late-time expansion.

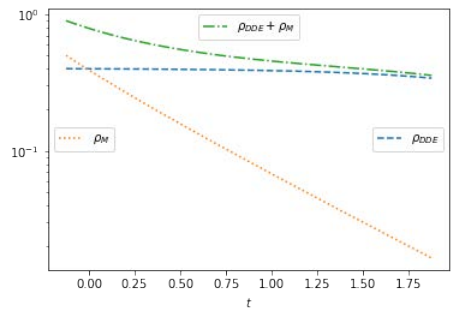

Figure 5. Case with $w_{DM} = 0$ and $w_{DDE} = 0.5$, showing a delayed approach to equality.

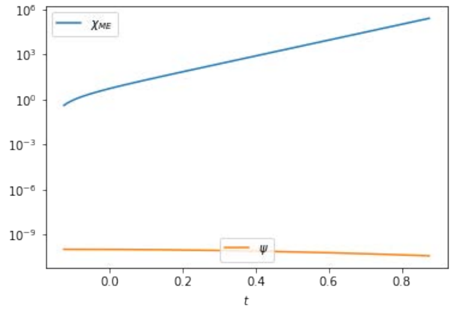

Figure 6. χ_{ME} as a function of cosmic time, with $\chi_{ME} = 1$ corresponding to $t_{eq} = 0$. The nearly linear growth suggests that χ_{ME} can be fixed in equation (24).

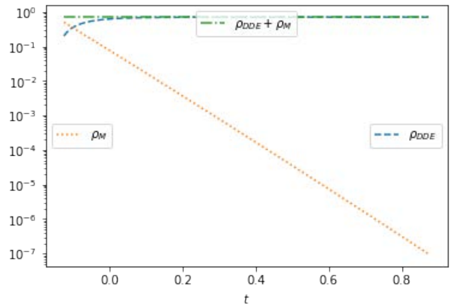

Figure 7. Accelerated expansion for $q = -1$. Using (24), one reconstructs $\omega_{DDE} = -2$, which lies in the phantom regime [47] at $\chi_{ME} = 1$.

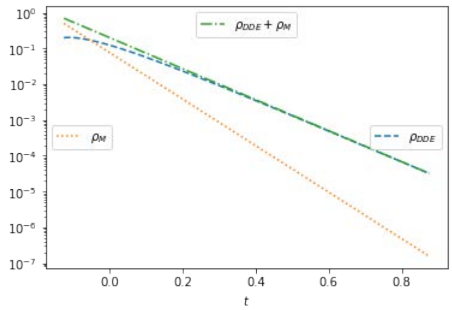

Figure 8. For $q = 0$, the dynamic dark energy density decreases with expansion, behaving similarly to baryonic matter with an equivalent $\omega_{DDE} = -2/3$.

Second, the same parameters are examined while varying q. The results, displayed in Figures 6, 7, 8, 9, and 10, highlight the sensitivity of the transition dynamics to the deceleration parameter.

7 Discussion and Conclusion

A key result of this study is the derivation of a new expression for the EoS of dynamic dark energy, written in terms of the density ratio between successive dominant components:

$$\omega_{DDE} = \frac{(2q-1)(1+\chi_{ME})}{3\chi_{ME}}, \tag{31}$$

where q is the deceleration parameter and χ_{ME} denotes the ratio of dynamic dark energy density to matter

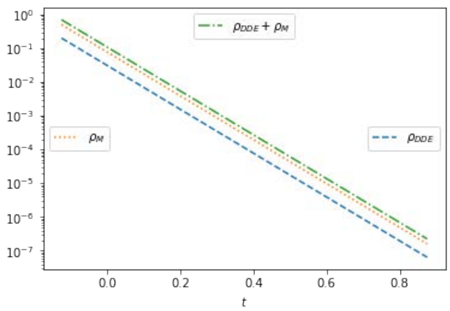

Figure 9. At $q = 0.5$, no crossover occurs: dynamic dark energy remains subdominant throughout.

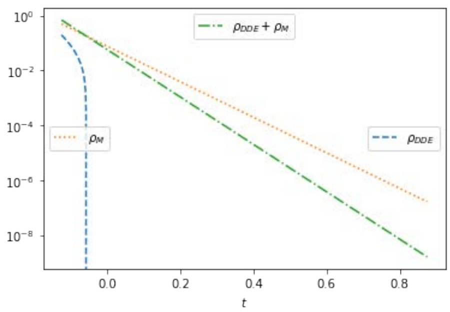

Figure 10. For $q = 1$, the dynamic dark energy density decays exponentially, preventing any crossover.

density. Because the Hubble parameter is not precisely determined, uncertainty in H propagates to q and hence to ω_{DDE}. Even so, numerical integration of the coupled density evolution equations points to $\omega_{DDE} < -2/3$ as the condition for accelerated expansion at the crossover $\chi_{ME} = 1$. The range $-1 < \omega_{DDE} < -2/3$ corresponds to the quintessence regime [48].

Recent analyses comparing different EoS parameterizations with observational data [49] suggest that ΛCDM and wCDM remain favoured according to the Bayesian Information Criterion (BIC). This does not eliminate dynamic dark energy as a possibility, but it does constrain the range of viable models. Furthermore, the continuing debate surrounding the Hubble tension underscores the importance of probing dark energy models through their EoS.

Data Availability Statement

Data will be made available on request.

Funding

This work was supported by the University of Cape Town's NGP.

Conflicts of Interest

The author declares no conflicts of interest.

Ethical Approval and Consent to Participate

Not applicable.

References

[1] Weinberg, D. H., Mortonson, M. J., Eisenstein, D. J., Hirata, C., Riess, A. G., & Rozo, E. (2013). Observational probes of cosmic acceleration. *Physics reports, 530*(2), 87-255. [CrossRef]

[2] Force, D. E. T. (2006). Report of the dark energy task force. *Available online from NSF*.

[3] Riess, A. G., Filippenko, A. V., Challis, P., Clocchiatti, A., Diercks, A., Garnavich, P. M., ... & Tonry, J. (1998). Observational evidence from supernovae for an accelerating universe and a cosmological constant. *The astronomical journal, 116*(3), 1009. [CrossRef]

[4] Lahav, O., & Liddle, A. R. (2004). The cosmological parameters. *arXiv preprint astro-ph/0406681*.

[5] Hinshaw, G., Larson, D., Komatsu, E., Spergel, D. N., Bennett, C., Dunkley, J., ... & Wright, E. L. (2013). Nine-year Wilkinson Microwave Anisotropy Probe (WMAP) observations: cosmological parameter results. *The Astrophysical Journal Supplement Series, 208*(2), 19. [CrossRef]

[6] Aghanim, N., Akrami, Y., Ashdown, M., Aumont, J., Baccigalupi, C., Ballardini, M., ... & Roudier, G. (2020). Planck 2018 results-VI. Cosmological parameters. *Astronomy & Astrophysics, 641*, A6. [CrossRef]

[7] Riess, A. G., Casertano, S., Yuan, W., Macri, L., Bucciarelli, B., Lattanzi, M. G., ... & Anderson, R. I. (2018). Milky Way Cepheid standards for measuring cosmic distances and application to Gaia DR2: implications for the Hubble constant. *The Astrophysical Journal, 861*(2), 126. [CrossRef]

[8] Riess, A. G., Anand, G. S., Yuan, W., Casertano, S., Dolphin, A., Macri, L. M., ... & Anderson, R. I. (2024). JWST observations reject unrecognized crowding of Cepheid photometry as an explanation for the Hubble tension at 8σ confidence. *The Astrophysical Journal Letters, 962*(1), L17. [CrossRef]

[9] Cunnington, S. (2022). Detecting the power spectrum turnover with H i intensity mapping. *Monthly Notices of the Royal Astronomical Society, 512*(2), 2408-2425. [CrossRef]

[10] Eisenstein, D. J., & Hu, W. (1998). Baryonic features in the matter transfer function. *The Astrophysical Journal, 496*(2), 605. [CrossRef]

[11] Dodelson, S., & Schmidt, F. (2020). *Modern cosmology*. Academic press.

[12] Vagnozzi, S. (2020). New physics in light of the H_0

tension: An alternative view. *Physical Review D*, *102*(2), 023518. [CrossRef]

[13] Birrer, S., Treu, T., Rusu, C. E., Bonvin, V., Fassnacht, C. D., Chan, J. H. H., ... & Meylan, G. (2019). H0LiCOW–IX. Cosmographic analysis of the doubly imaged quasar SDSS 1206+ 4332 and a new measurement of the Hubble constant. *Monthly Notices of the Royal Astronomical Society*, *484*(4), 4726-4753. [CrossRef]

[14] Knox, L., & Millea, M. (2020). Hubble constant hunter's guide. *Physical Review D*, *101*(4), 043533. [CrossRef]

[15] Chamings, F. N., Avgoustidis, A., Copeland, E. J., Green, A. M., & Pourtsidou, A. (2020). Understanding the suppression of structure formation from dark matter-dark energy momentum coupling. *Physical Review D*, *101*(4), 043531. [CrossRef]

[16] Mortonson, M. J., Weinberg, D. H., & White, M. (2013). Dark energy: a short review. *arXiv preprint arXiv:1401.0046*.

[17] Tsujikawa, S. (2011). Dark energy: investigation and modeling. In *Dark Matter and Dark Energy: A Challenge for Modern Cosmology* (pp. 331-402). Dordrecht: Springer Netherlands. [CrossRef]

[18] Li, M., Li, X. D., Wang, S., & Wang, Y. (2011). Dark energy. *Communications in theoretical physics*, *56*(3), 525. [CrossRef]

[19] Weinberg, S. (2013). *Gravitation and cosmology: principles and applications of the general theory of relativity*. John Wiley & Sons. [CrossRef]

[20] Peebles, P. J. E. (1993). *Principles of physical cosmology*. Princeton University Press.

[21] Tian, S. (2017). The relation between cosmological redshift and scale factor for photons. *The Astrophysical Journal*, *846*(2), 90. [CrossRef]

[22] Perlmutter, S., Aldering, G., Goldhaber, G., Knop, R. A., Nugent, P., Castro, P. G., ... & Supernova Cosmology Project. (1999). Measurements of Ω and Λ from 42 high-redshift supernovae. *The Astrophysical Journal*, *517*(2), 565–586. [CrossRef]

[23] Maartens, R. (1996). Causal thermodynamics in relativity. *arXiv:astro-ph/9609119*.

[24] Israel, W. (2009). Relativistic thermodynamics. In *ECG Stueckelberg, An Unconventional Figure of Twentieth Century Physics: Selected Scientific Papers with Commentaries* (pp. 101-113). Basel: Birkhäuser Basel. [CrossRef]

[25] Israel, W., & Stewart, J. M. (1979). Transient relativistic thermodynamics and kinetic theory. *Annals of Physics*, *118*(2), 341-372. [CrossRef]

[26] Hiscock, W., & Lindblom, L. (1983). Stability and causality in dissipative relativistic fluids. *Annals of Physics*, *151*(2), 466–496. [CrossRef]

[27] Osano, B. (2020). The thermodynamics of relativistic multifluid systems. *Letters in High Energy Physics*, *2020*(141), 1–8. [CrossRef]

[28] Barkana, R. (2018). Possible interaction between baryons and dark-matter particles revealed by the first stars. *Nature*, *555*(7694), 71–74. [CrossRef]

[29] Osano, B. (2020). Evolution of cosmological total energy density and transient periods in cosmology. *arXiv preprint arXiv:2002.08875*.

[30] Osano, B. (2025). Dark energy: A dynamical systems approach to the reconstruction of the equation of state. *Journal of Mathematical Physics*, *66*(9). [CrossRef]

[31] Bahr-Kalus, B., Parkinson, D., & Mueller, E. M. (2023). Measurement of the matter-radiation equality scale using the extended baryon oscillation spectroscopic survey quasar sample. *Monthly Notices of the Royal Astronomical Society*, *524*(2), 2463-2476. [CrossRef]

[32] Hu, W., & Sugiyama, N. (1995). Small scale cosmological perturbations: An analytic approach. *The Astrophysical Journal*, *471*(2), 542–570. [CrossRef]

[33] Chevallier, M., & Polarski, D. (2001). Accelerating universes with scaling dark matter. *International Journal of Modern Physics D*, *10*(02), 213-223. [CrossRef]

[34] Linder, E. V. (2008). The dynamics of quintessence, the quintessence of dynamics. *General Relativity and Gravitation*, *40*(2), 329–356. [CrossRef]

[35] Barboza Jr, E. M., & Alcaniz, J. S. (2008). A parametric model for dark energy. *Physics Letters B*, *666*(5), 415–419. [CrossRef]

[36] Wang, Y. (2008). Figure of merit for dark energy constraints from current observational data. *Physical Review D*, *77*(12), 123525. [CrossRef]

[37] Bouali, A., Chaudhary, H., Debnath, U., Sardar, A., & Mustafa, G. (2023). Data analysis of three parameter models of deceleration parameter in FLRW universe. *The European Physical Journal Plus*, *138*(9), 1-26. [CrossRef]

[38] Alam, U., Sahni, V., Deep Saini, T., & Starobinsky, A. A. (2004). Is there supernova evidence for dark energy metamorphosis?. *Monthly Notices of the Royal Astronomical Society*, *354*(1), 275-291. [CrossRef]

[39] Alam, U., Sahni, V., & Starobinsky, A. A. (2004). The case for dynamical dark energy revisited. *Journal of Cosmology and Astroparticle Physics*, *2004*(06), 008. [CrossRef]

[40] Escamilla-Rivera, C. & Nájera, A. (2022). Dynamic dark energy models in the light of Gravitational-Wave Transient Catalogues. *Journal of Cosmology and Astroparticle Physics*, *2022*(03), 060. [CrossRef]

[41] Kundu, R., Debnath, U., & Pradhan, A. (2023). Studying the optical depth behavior of parametrized deceleration parameter in non-flat universe. *International Journal of Geometric Methods in Modern Physics*, *20*(07), 2350110. [CrossRef]

[42] Pourojaghi, S., & Malekjani, M. (2021). A new comparison between holographic dark energy and

standard Λ-cosmology in the context of cosmography method. *The European Physical Journal C*, *81*(7), 575. [CrossRef]

[43] Wei, H., Yan, X. P., & Zhou, Y. N. (2014). Cosmological applications of Pade approximant. *Journal of Cosmology and Astroparticle Physics*, *2014*(01), 045. [CrossRef]

[44] Rezaei, M., Malekjani, M., Basilakos, S., Mehrabi, A., & Mota, D. F. (2017). Constraints to dark energy using PADE parameterizations. *The Astrophysical Journal*, *843*(1), 65. [CrossRef]

[45] Frieman, J. A., Turner, M. S., & Huterer, D. (2008). Dark energy and the accelerating universe. *Annu. Rev. Astron. Astrophys.*, *46*(1), 385-432. [CrossRef]

[46] Kopp, M., Skordis, C., Thomas, D. B., & Ilić, S. (2018). Dark matter equation of state through cosmic history. *Physical Review Letters*, *120*(22), 221102. [CrossRef]

[47] Li, M., Qiu, T., Cai, Y., & Zhang, X. (2012). On dark energy models of single scalar field. *Journal of Cosmology and Astroparticle Physics*, *2012*(04), 003. [CrossRef]

[48] Caldwell, R. R., Doran, M., Müller, C. M., Schäfer, G., & Wetterich, C. (2003). Early quintessence in light of the Wilkinson Microwave Anisotropy Probe. *The Astrophysical Journal*, *591*(2), L75. [CrossRef]

[49] Rahman, S. F. (2020). Dynamic dark energy equation of state (EoS) and Hubble constant analysis using type Ia supernovae from Union 2.1 dataset. *Astronomy Reports*, *64*(4), 354–367. [CrossRef]

Bob Osano received the PhD. degree in Applied Mathematics from the University of Cape Town, Cape Town, South Africa, in 2008. His research interests include perturbations theory, general relativity and cosmology. (Email: bob.osano@uct.ac.za)